

000 001 002 003 004 005 006 007 008 009 010 011 012 013 014 015 016 017 018 019 020 021 022 023 024 025 026 027 028 029 030 031 032 033 034 035 036 037 038 039 040 041 042 043 044 045 046 047 048 049 050 051 052 053 EXPERT HEADS: ROBUST EVIDENCE IDENTIFICATION FOR LARGE LANGUAGE MODELS

Anonymous authors

Paper under double-blind review

ABSTRACT

Large language models (LLMs) exhibit strong abilities in multi-document reasoning, yet their evidence identification is highly sensitive to input order. We trace this limitation to attention mechanisms, where many heads overemphasize sequence boundaries and neglect central content. We systematically analyze attention distributions under document permutations and discover a small subset of heads that consistently prioritize task-relevant documents regardless of position. We formalize these as **Expert Heads**, identified via activation frequency and stability across permutations. Experiments on LLaMA, Mistral, and Qwen reveal architecture-specific patterns: mid-layer heads in LLaMA and Mistral dominate semantic integration, while deeper-layer heads in Qwen specialize in evidence selection. Moreover, Expert Heads exhibit concentrated focus during understanding and more distributed engagement during generation. Their activation strongly correlates with answer correctness, providing diagnostic signals for hallucination detection. Leveraging Expert Heads for document voting significantly improves retrieval and ranking on HotpotQA, 2WikiMultiHopQA, and MuSiQue, outperforming dense retrievers and LLM-based ranking with minimal overhead. Ablations confirm that even a small subset achieves robust gains. Our findings establish Expert Heads as a stable and interpretable mechanism for evidence integration, offering new directions for context pruning, hallucination mitigation, and head-guided training of LLMs.¹

1 INTRODUCTION

Large language models (LLMs) exhibit strong capabilities in aggregating information across multiple documents (Lewis et al., 2020; Wei et al., 2022). Yet, their ability to identify task-relevant evidence is highly sensitive to input order (Liu et al., 2023; Zheng et al., 2023; Pezeshkpour & Hruschka, 2023). This positional sensitivity largely stems from attention mechanisms: many heads overemphasize sequence boundaries and fail to consistently capture critical content in the middle of the context (Press et al., 2021; Guo et al., 2024; Wu et al., 2025). Addressing this limitation requires a deeper understanding of how attention distributes across documents and which components are truly responsible for robust evidence integration.

To this end, we systematically examine LLM attention under context permutations. As shown in Fig. 1, in each model, a small set of attention heads consistently attend to gold documents regardless of their position. These heads appear to play a unique role in identifying task-critical evidence and exhibit resilience to positional variations. This raises an important question: *can we reliably identify such heads and leverage them to enhance both robustness and interpretability?*

We build on this observation by introducing a framework to isolate these heads. We define **Activated Heads** as those that allocate more attention to all gold documents than to distractors, thereby avoiding the pitfalls of naive top-attention selection. We then quantify their stability across permutations and designate the most reliable and focused subset as **Expert Heads**.

Our analysis reveals deeper insights into LLM internal organization. Expert Heads follow distinct layer-wise distributions across architectures: in LLaMA and Mistral, mid-layer heads dominate

¹Our code, dataset, and the models used in this work are available at <https://anonymous.4open.science/r/ExpertHead/>

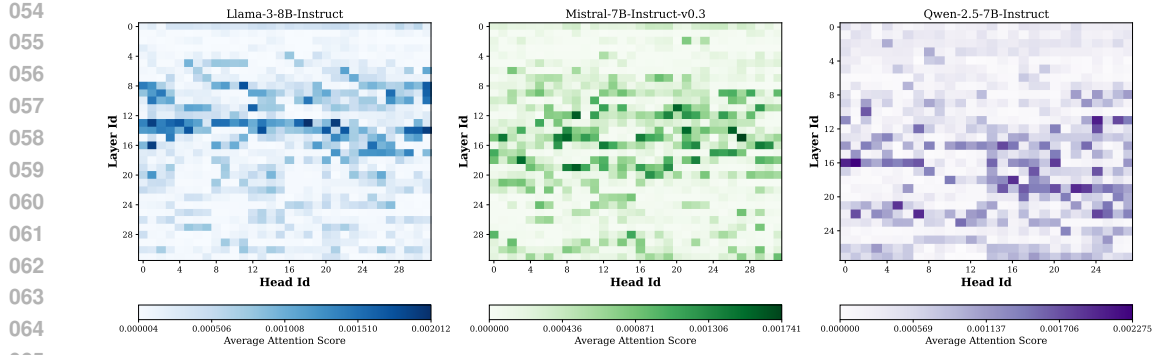


Figure 1: Head-wise distribution of average attention scores for gold documents across three LLMs. Scores are computed by averaging over input permutations where gold documents appear in different positions. Each subplot presents all heads across layers, with color intensity representing the average score assigned to gold documents. The heatmaps highlight a small subset of heads that consistently allocate strong attention to gold documents, indicating their potential role as Expert Heads. Distinct color maps are used for clarity across models.

semantic integration, while in Qwen, deeper-layer heads specialize in evidence selection, highlighting architecture-specific alignment strategies. Moreover, under *Query-as-Source* and *Response-as-Source* attention, more heads participate during answer generation, and their focus is slightly more dispersed, indicating functional shifts across decoding stages.

Through extensive experiments, we show that Expert Heads are closely linked to model performance. When the model produces correct answers, these heads activate more frequently and focus on task-relevant evidence. Conversely, when the model makes errors, their activation weakens or spreads out, leading to insufficient evidence integration and occasional hallucinations. Leveraging Expert Heads for document voting consistently improves identification and ranking across multiple benchmarks (Yang et al., 2018; Ho et al., 2020; Trivedi et al., 2022), outperforming standard retrieval pipelines and direct LLM-based ranking.

In summary, Expert Heads provide a stable, interpretable, and efficient mechanism for evidence integration, revealing LLM internal reasoning patterns, layer-specific roles, and practical utility for improving document identification and ranking.

2 ATTENTION HEAD ACTIVATION

To investigate how large language models (LLMs) dynamically allocate attention to task-relevant evidence during context understanding and answer generation, this section analyzes the activation patterns of attention heads under different document permutations.

2.1 PRELIMINARIES

Input Construction and Permutations. Given a query Q , a set of m distractor documents $\{D_1, D_2, \dots, D_m\}$, and n gold documents $\{G_1, G_2, \dots, G_n\}$, we construct multiple input permutations to systematically evaluate the effect of document order on attention head behavior. Each input sequence consists of a task instruction, all distractor documents, and the query, with gold documents inserted at different positions among the distractors. Instead of enumerating all possible permutations, we only vary the insertion positions of gold documents relative to distractors. This results in $m + 1$ permutations per query, ensuring that every gold document appears in all possible positions within the context.

Attention Sources. For any document $D \in \{G_1, \dots, G_n, D_1, \dots, D_m\}$, We consider two types of attention sources:

108 *Query-as-Source*: Attention from query tokens Q to document D , reflecting the model’s estimation
 109 of relevance during context understanding:
 110

$$111 \quad A_{Q \rightarrow D}^{(l,h)} = \frac{1}{|Q| \cdot |D|} \sum_{q \in Q} \sum_{d \in D} A_{q,d}^{(l,h)}. \quad (1)$$

113 *Response-as-Source*: Attention from generated response tokens R to document D , capturing the
 114 evidence actually utilized during answer generation:
 115

$$116 \quad A_{R \rightarrow D}^{(l,h)} = \frac{1}{|R| \cdot |D|} \sum_{r \in R} \sum_{d \in D} A_{r,d}^{(l,h)}. \quad (2)$$

119 Together, these two perspectives provide a comprehensive view: Query-as-Source indicates which
 120 content the model deems important, while Response-as-Source reveals how that content is subse-
 121 quently used in generation.

122 **Activated Heads.** For each permutation π and attention source $src \in Q, R$, an attention head (l, h)
 123 is considered *activated* if it attends more strongly to all gold documents than to any distractor:

$$125 \quad \text{Activated}(l, h)_{src}^{\pi} = \begin{cases} 1, & \text{if } A_{src \rightarrow G_j}^{(l,h)} > A_{src \rightarrow D_i}^{(l,h)}, \forall j \in \{1, \dots, n\}, \forall i \in \{1, \dots, m\}, \\ 126 & 0, \text{ otherwise.} \end{cases} \quad (3)$$

128 This stricter criterion avoids biases from naive top-attention selection, where some heads might
 129 appear highly activated due to positional effects rather than true relevance to the task.

130 2.2 ATTENTION ANALYSIS SETUP

132 **Models.** We conduct experiments on three widely used instruction-tuned LLMs: LLaMA-3-8B-
 133 Instruct (Patterson et al., 2022) (32 layers, 32 attention heads per layer), Mistral-7B-Instruct-
 134 v0.3 (AI, 2024) (32 layers, 32 heads per layer), and Qwen-2.5-7B-Instruct (Yang et al., 2024; Team,
 135 2024) (28 layers, 28 heads per layer). These models offer sufficiently rich attention structures to
 136 enable fine-grained head-level interpretability.

137 **Dataset.** For reproducibility, we randomly sample 5,000 instances from the HotpotQA (Yang et al.,
 138 2018) train set, each containing two gold and eight distractor documents, yielding nine permutations
 139 per query. This results in **45,000 input instances per model**, providing a comprehensive basis for
 140 analyzing attention behaviors under systematically varied document positions.

142 **Attention Extraction.** For each input instance, we extract attention maps from all heads across all
 143 layers. Both Query-as-Source and Response-as-Source attention matrices are computed using Eqs. 1
 144 and 2. The binary activation status of each head is then determined using Eq. 3. This setup enables
 145 head-wise analysis of how attention distribution depends on document ordering.

146 2.3 ACTIVATION PATTERNS OF ATTENTION HEADS

148 Figure 2 shows that gold documents placed at boundary positions (beginning or end of the context)
 149 trigger a larger number of activated heads, but with relatively weaker attention scores. In contrast,
 150 gold documents located in the middle elicit fewer activated heads, yet with stronger and more fo-
 151 cused attention.

152 This positional effect is also reflected in performance: as shown in Appendix Fig. 7, multi-hop QA
 153 accuracy is highest when gold documents appear at the start or end, but drops when they occur in the
 154 middle. This demonstrates that both attention allocation and downstream performance are sensitive
 155 to document position.

156 We further observe notable differences between attention sources. With Query-as-Source, fewer
 157 heads are activated, but their average scores are higher, suggesting that a small set of heads suffices
 158 to capture task-critical semantics. With Response-as-Source, more heads are engaged, but their
 159 attention is more dispersed, indicating a broader integration of evidence during answer generation.

161 Overall, these findings highlight that LLMs dynamically adjust their attention allocation strategies
 162 depending on the stage of processing and the position of critical evidence within the context.

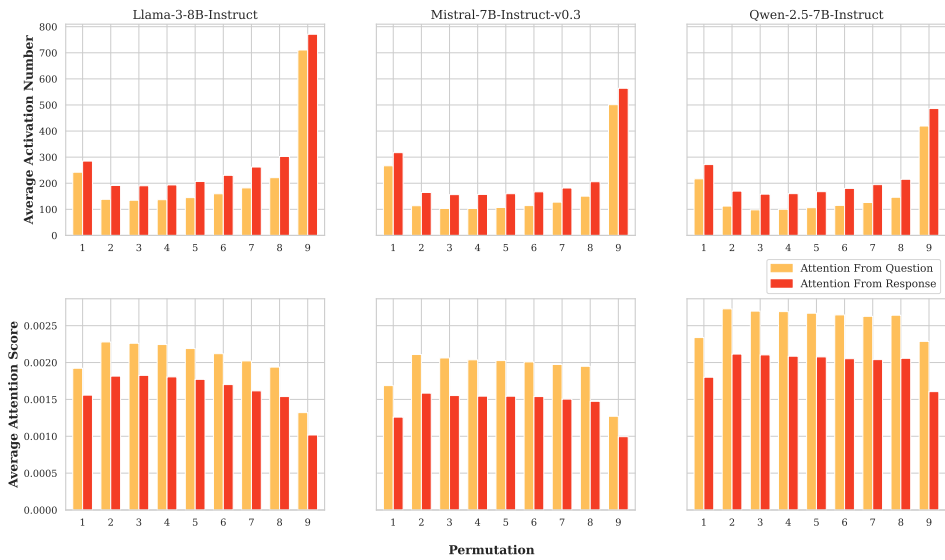


Figure 2: Number of activated heads (top) and average attention scores (bottom) across different gold document permutations. Gold documents at boundary positions activate more heads but with weaker attention, whereas middle positions activate fewer heads but with stronger, more focused attention. The x-axis (1–9) denotes the gold document position within the context, from start (1) to end (9).

3 EXPERT HEAD IDENTIFICATION

Building on the activation patterns observed in Sec. 2, this section analyzes the behavior of activated heads to identify those that consistently demonstrate stability and strong focus on gold documents across different document permutations.

3.1 DEFINITION

To quantify the reliability and importance of individual attention heads, we introduce two complementary statistics:

Activation Frequency $f_{\pi}^{(l,h)}$: measures the proportion of samples in which a head (l, h) is activated under permutation π , reflecting its consistency:

$$f_{\pi}^{(l,h)} = \frac{1}{|\mathcal{S}|} \sum_{s \in \mathcal{S}} \text{Activated}(l, h)_{src}^{\pi,s}. \quad (4)$$

Here, \mathcal{S} denotes the set of all input samples.

Average Attention Score $\bar{A}_{\pi}^{(l,h)}$: measures the mean attention allocated by head (l, h) to gold documents across activated samples, reflecting its ability to concentrate on task-relevant information:

$$\bar{A}_{\pi}^{(l,h)} = \frac{\sum_{s \in \mathcal{S}} \text{Activated}(l, h)_{src}^{\pi,s} \cdot \sum_{j=1}^n A_{src \rightarrow G_j}^{(l,h),s}}{\sum_{s \in \mathcal{S}} \text{Activated}(l, h)_{src}^{\pi,s}}. \quad (5)$$

To systematically evaluate activated heads, we adopt two thresholds: (1) **Activation frequency threshold** $\tau_f = 0.6$, requiring that a head be activated in more than 60% of samples under a given permutation. (2) **Average attention score percentile** $\tau_p = 0.9$, retaining only the top 10% of activated heads ranked by average attention to gold documents. These thresholds strike a balance between reliability (frequent activation) and focus (strong attention to evidence).

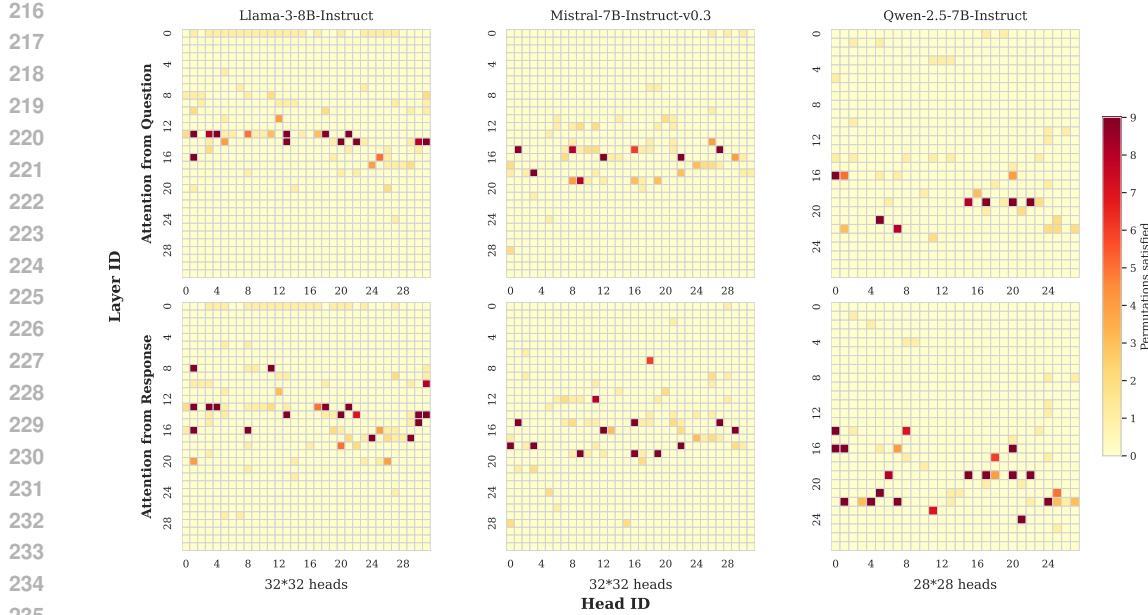


Figure 3: Distribution of Sensitive Heads across layers and head indices. Top: Question-as-Source; Bottom: Response-as-Source. Color intensity reflects the number of permutations in which a head satisfies the Sensitive Head criteria, with darker shades indicating higher consistency. Expert Heads, which satisfy criteria across all permutations, appear in the darkest color.

Sensitive and Expert Heads. An Activated head is classified as a **Sensitive Head** if it satisfies both thresholds for *at least one permutation*:

$$\text{SensitiveHeads} = \left\{ (l, h) \mid \exists \pi, f_{\pi}^{(l,h)} > \tau_f \wedge \bar{A}_{\pi}^{(l,h)} > P\tau_p(\bar{A}_{\pi}^{(l',h')}) \right\}. \quad (6)$$

A Sensitive Head is further promoted to an **Expert Head** if it consistently meets both thresholds across *all permutations*:

$$\text{ExpertHeads} = \left\{ (l, h) \mid \forall \pi, f_{\pi}^{(l,h)} > \tau_f \wedge \bar{A}_{\pi}^{(l,h)} > P\tau_p(\bar{A}_{\pi}^{(l',h')}) \right\}. \quad (7)$$

The full selection procedure is summarized in Alg. 1 in Appendix C.

3.2 EXPERT HEAD ANALYSIS

Figure 3 illustrates the distribution of Sensitive Heads across model layers and head indices. For LLaMA-3-8B-Instruct and Mistral-7B-Instruct-v0.3, Sensitive Heads are concentrated in middle layers, underscoring the role of these layers in semantic integration. In contrast, Qwen-2.5-7B-Instruct exhibits a greater concentration of Sensitive Heads in deeper layers, suggesting that later layers specialize in evidence selection.

Among these Sensitive Heads, those that remain consistently active across all permutations are identified as **Expert Heads**. Figure 4 shows that, under Query-as-Source, Expert Heads form a smaller but more focused subset of the broader pool engaged under Response-as-Source. This indicates that, while answer generation involves a larger set of heads for evidence integration, Expert Heads retain sharper focus on task-relevant documents.

Figure 5 further demonstrates the relationship between Expert Head activation and model answer correctness. When answers are correct, Expert Heads show both higher activation frequencies and stronger average attention scores on gold documents. Conversely, when answers are incorrect, Expert Head activation is weaker and their attention becomes more dispersed, leading to poorer evidence integration and an increased risk of hallucination.

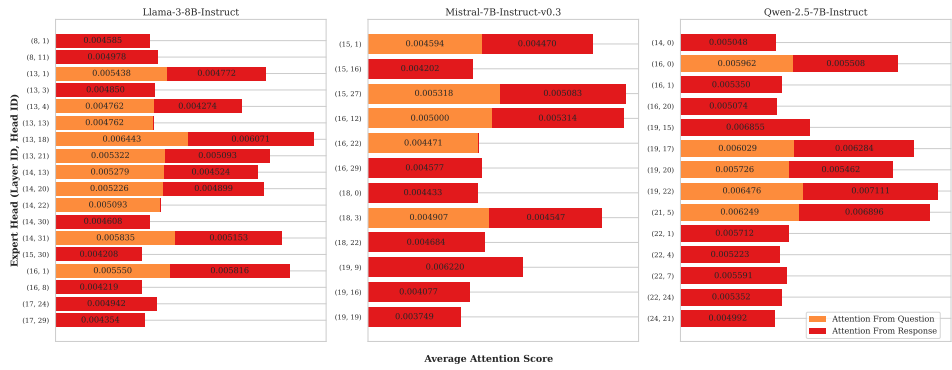


Figure 4: Head-wise distribution of Expert Heads and their average attention scores. Horizontal stacked bars show contributions from Question-as-Source (orange) and Response-as-Source (red). The concentration of Expert Heads differs across models, reflecting distinct layer-specific roles in semantic integration and evidence selection.

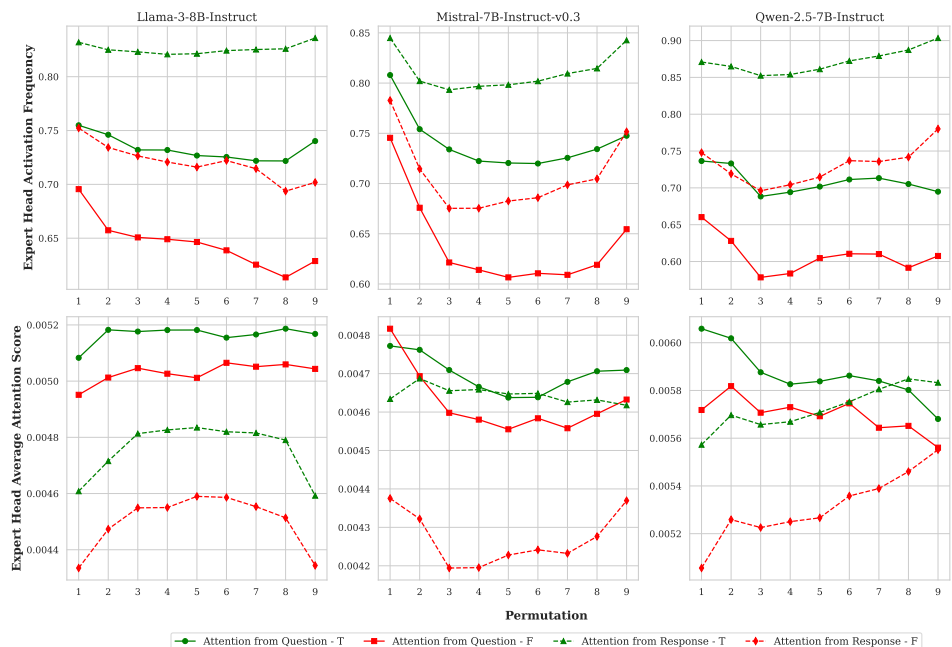


Figure 5: Relationship between Expert Head activation and model answer correctness. Green curves denote correct answers, red curves incorrect ones; solid lines represent Question-as-Source, dashed lines Response-as-Source. Top: activation frequency; Bottom: average attention score. Expert Heads are more active and concentrated in correct cases, while weaker or dispersed activation correlates with errors. The x-axis (1–9) indicates the gold document’s position, from beginning (1) to end (9).

4 EVALUATION OF EXPERT HEADS

We evaluate the practical effectiveness of Expert Heads on **document identification and ranking tasks**, rather than directly on QA accuracy. Conventional QA evaluation relies on metrics such as answer correctness or string matching, which may obscure whether a model actually attends to task-relevant evidence. Performance can also be influenced by components beyond attention (e.g., feed-forward layers or decoding strategies), making it difficult to isolate the contribution of evidence integration. In contrast, document identification and ranking provide a more controlled

324
 325 Table 1: Precision@2 (P@2), NDCG@2, and MAP performance across three datasets. Each base
 326 model includes three variants: Expert Heads (Question), Expert Heads (Response), and LLM Rank.
 327 Baselines include BM25, DPR, Contriever, MiniLM, GTR, ColBERTv2, BGE, and Qwen3. Best
 328 results are shown in **bold**; second-best are underlined.

Method	HotpotQA			2WikiMultiHopQA			MuSiQue		
	P@2	NDCG@2	MAP	P@2	NDCG@2	MAP	P@2	NDCG@2	MAP
BM25	57.47	50.23	<u>60.58</u>	52.77	45.64	56.80	49.30	43.27	54.66
DPR	60.14	52.97	63.17	61.27	54.85	64.79	58.61	50.82	61.50
Contriever	61.50	55.19	64.90	59.51	52.15	62.07	62.37	54.04	64.01
MiniLM	71.04	64.04	71.82	73.07	65.72	73.43	65.47	56.75	66.37
GTR	64.26	57.32	66.65	70.03	61.89	70.26	64.42	55.94	65.78
ColBERTv2	64.63	57.31	66.58	68.70	61.21	69.89	60.42	51.80	62.25
BGE	75.23	69.45	76.37	77.12	71.06	77.76	70.25	62.89	71.26
Qwen3	68.55	61.77	70.21	73.27	65.84	73.68	66.55	57.54	67.05
LLaMA-3-8B-Instruct									
Expert Heads (Q)	88.23	89.97	94.03	73.47	77.84	85.71	82.18	84.78	90.08
Expert Heads (R)	90.72	91.98	95.08	<u>77.30</u>	<u>81.58</u>	<u>87.83</u>	83.57	86.05	90.95
LLM Rank	66.31	70.06	78.22	<u>76.49</u>	<u>79.65</u>	<u>86.60</u>	69.63	73.70	80.93
Mistral-7B-Instruct-v0.3									
Expert Heads (Q)	88.08	89.73	93.60	70.72	75.27	83.21	80.03	82.98	88.76
Expert Heads (R)	<u>88.89</u>	<u>90.50</u>	<u>94.13</u>	73.27	77.62	84.83	80.53	83.40	88.85
LLM Rank	36.45	39.97	55.03	45.14	49.82	62.22	39.72	44.31	57.54
Qwen-2.5-7B-Instruct									
Expert Heads (Q)	86.93	88.69	93.19	74.69	78.47	85.72	81.30	83.85	89.44
Expert Heads (R)	88.45	90.02	93.87	77.94	81.88	88.29	<u>82.70</u>	<u>85.02</u>	<u>90.11</u>
LLM Rank	77.81	78.70	86.11	76.57	80.89	87.15	<u>76.65</u>	79.68	88.97

350
 351 and interpretable setting, allowing us to directly assess whether Expert Heads reliably focus on
 352 critical documents.

354 355 4.1 EXPERIMENTAL SETTING

356
 357 **Task Definition.** Given a query Q , two gold documents $\{G_1, G_2\}$, and eight distractor documents
 358 $\{D_1, \dots, D_8\}$, the model must identify and rank the gold documents among all candidates. We evaluate
 359 performance using both identification-oriented metrics (**Precision@2**) and ranking-oriented
 360 metrics (**NDCG@2** and **MAP**) to provide a comprehensive assessment.

361
 362 **Datasets.** Experiments are conducted on the test sets of HotpotQA (2269 samples), 2WikiMultiHopQA
 363 (Ho et al., 2020) (2471 samples), and MuSiQue (Trivedi et al., 2022) (2486 samples),
 364 providing diverse scenarios for evaluating document identification and ranking.

365
 366 **Document Ranking with Expert Head Voting.** We evaluate Expert Heads derived from both
 367 Query-as-Source and Response-as-Source attention across LLaMA-3-8B-Instruct, Mistral-7B-
 368 Instruct-v0.3, and Qwen-2.5-7B-Instruct. For each model and each attention source, we first select
 369 Expert Heads based on activation frequency τ_f and average attention score percentile τ_p , fixing the
 370 number of Expert Heads at **five per setting** to ensure fairness.

371 Given a query and candidate documents, each Expert Head independently produces a ranking based
 372 on its attention scores *from the query to each candidate*. Final rankings are then aggregated through
 373 a **voting scheme** across the five Expert Heads. Details of the thresholds and voting procedure are
 374 provided in Appendix B and C.

375
 376 **Baselines.** We compare Expert Heads against widely used retrieval models: BM25 (Robertson
 377 et al., 2009), DPR (Karpukhin et al., 2020), Contriever (Izacard et al., 2021), MiniLM (Wang et al.,
 378 2020), GTR (Ni et al., 2021), ColBERTv2 (Santhanam et al., 2021), BGE (Xiao et al., 2024),
 379 Qwen3 (Zhang et al., 2025) and LLM Rank, which refers to direct document ranking by model
 380 generation.

378
379

4.2 MAIN RESULTS

380
381
382
383
384
385

As shown in Table 1, experimental results demonstrate that Expert Heads substantially surpass all baseline retrieval models across all datasets, indicating their effectiveness in document ranking tasks. Importantly, they provide a principled and interpretable mechanism for document ranking. By focusing on a small, consistently activated subset of heads, they highlight the model components most responsible for evidence integration, offering insights into reasoning patterns without relying on black-box full-model outputs.

386
387

4.3 ABLATION STUDY

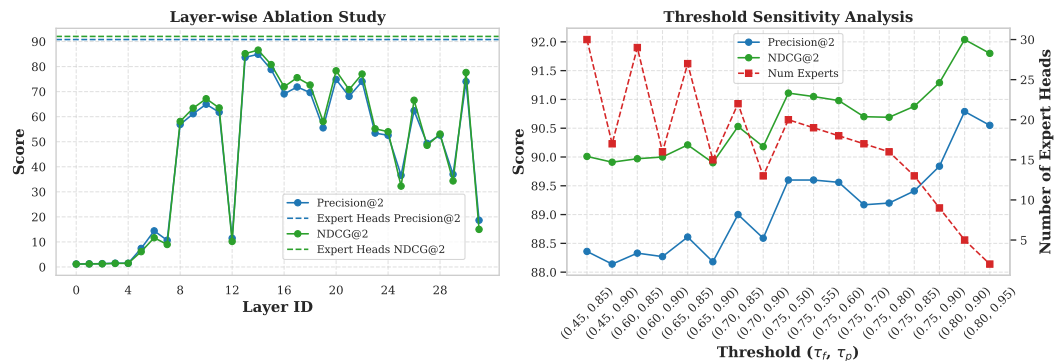
388
389
390
391
392
393
394
395
396
397
398
399
400
401402
403
404
405
406
407

Figure 6: Ablation study results. Left: Layer-wise ablation, where all heads within one layer are treated as Expert Heads. Results show that middle layers contribute most, while lower layers play a limited role and final layers degrade performance. Right: Threshold sensitivity for Response-as-Source Expert Heads across varying activation thresholds. Performance improves under stricter criteria, even though the number of selected heads decreases sharply, indicating that tighter thresholds yield more specialized and effective subsets.

408
409
410
411

As shown in Fig. 6, we further conduct ablation experiments to analyze layer contributions and threshold sensitivity on LLaMA-3-8B-Instruct using the HotpotQA test set (2323 samples), with Precision@2 and NDCG@2 as evaluation metrics.

412
413
414
415
416
417

Layer-wise Ablation. We evaluate the contribution of different layers by treating all heads from a given layer as expert heads. Results reveal that middle layers contribute the most to performance, confirming their critical role in semantic integration and evidence selection, while lower layers play a limited role. Interestingly, using the final layer for document identification and ranking leads to a significant drop in performance, possibly because the model is already focused on preparing to generate the next token.

418
419
420
421
422
423
424

Threshold Sensitivity. We further analyze the effect of varying activation thresholds on Response-as-Source expert heads. As thresholds become stricter, the number of selected expert heads decreases substantially. Interestingly, instead of degrading, performance gradually improves under stricter criteria. This indicates that higher thresholds effectively filter out less informative heads, leaving a smaller yet more specialized subset that contributes more strongly to evidence identification and ranking. Thus, Expert Heads not only remain robust to threshold selection but can even benefit from tighter activation constraints.

425
426
427

5 DISCUSSIONS

428
429
430
431

Expert Heads provide a natural signal for context reranking, pruning, and interpretability. Because they consistently highlight task-critical evidence, their attention patterns can guide context reranking by moving highly attended documents closer to the end of the context, or context pruning by discarding distractors that receive negligible attention. This head-guided mechanism reduces computational cost in long-context settings while preserving reasoning quality. In addition, Expert

432 Heads make the model’s reasoning process more interpretable: instead of black-box ranking scores,
 433 users can directly observe which documents are prioritized by the most reliable heads, yielding
 434 transparent explanations for model outputs.

435 **Expert Heads offer a principled approach to hallucination mitigation and factuality detection.**
 436 Our experiments show that correct answers are associated with stronger and more concentrated Ex-
 437 pert Head activations, while incorrect answers display weaker or dispersed activation. This suggests
 438 that activation strength and focus can be used as a diagnostic signal to detect hallucinations in real
 439 time. Responses accompanied by weak or diffuse Expert Head patterns can be flagged as unreliable,
 440 enabling factuality-aware decoding strategies that enforce tighter grounding of answers to verifiable
 441 evidence, particularly in multi-document reasoning scenarios.

442 **Expert Heads can also serve as guidance for model distillation and reinforcement learning.** In
 443 knowledge distillation, the attention maps of Expert Heads in a teacher model can be transferred to
 444 a student model, ensuring that evidence-centric reasoning is preserved during compression. In rein-
 445 forcement learning or Reinforcement Learning from Human Feedback (RLHF), Expert Head acti-
 446 vation can be incorporated into the reward function, encouraging models to prioritize task-relevant
 447 documents during reasoning. This bridges interpretability and training, providing a way to align
 448 model optimization not only with human preferences but also with evidence fidelity, ultimately
 449 leading to more reliable and controllable language models.

450 451 6 RELATED WORK

452 **Retrieval and Ranking Methods.** Retrieval has evolved from sparse term-based approaches to
 453 dense neural representations (Johnson et al., 2019; Khattab & Zaharia, 2020; Khattab et al., 2021a;b;
 454 Santhanam et al., 2022) and embeddings derived from large language models (Zhang et al., 2023;
 455 Xiao et al., 2023). Modern encoders prioritize efficiency and generalization, while recent open-
 456 source models (Li et al., 2023a; Zhang et al., 2024) enhance multilingual capabilities, instruction-
 457 following, and long-context handling. In parallel, LLM-based ranking methods directly leverage
 458 language models as rerankers (Zhuang et al., 2023; 2024a;b; Drozdzov et al., 2023), often achieving
 459 superior semantic matching and reasoning, albeit with higher computational cost.

460 **Functional Specialization and Interpretability of Attention Heads.** Early work (Jain & Wallace,
 461 2019; Clark et al., 2019) questioned whether raw attention weights provide faithful explanations,
 462 showing they can be misleading without controlled analysis. Later studies (Kovaleva et al., 2019;
 463 Vig, 2019) demonstrated that attention becomes informative when paired with interventions—e.g.,
 464 head ablation (Michel et al., 2019; Voita et al., 2019), attention-weight manipulation (Serrano &
 465 Smith, 2019; Wiegreffe & Pinter, 2019), causal probing (Pruthi et al., 2019), and counterfactual
 466 edits (Abnar & Zuidema, 2020)—which can identify heads that causally influence model behav-
 467 ior. More recent research (Li et al., 2023b; Kumar et al., 2024; Zheng et al., 2024) highlights
 468 functional specialization of specific heads—for example, induction heads (Ren et al., 2024), name-
 469 mover heads (Tigges et al., 2023; García-Carrasco et al., 2024). These findings support treating
 470 certain attention heads as mechanistic primitives that drive model behavior, enabling targeted inter-
 471 pretability and modification. Our work extends this line of inquiry by identifying Expert Heads as
 472 stable mechanisms for robust evidence integration.

473 474 7 CONCLUSION

475 In this work, we identify **Expert Heads**, a small subset of attention heads that consistently focus
 476 on task-critical evidence across permutations, models, and attention sources. Our findings reveal
 477 layer-specific functional specialization in LLMs: mid-layer heads in LLaMA and Mistral domi-
 478 nate semantic integration, while deeper-layer heads in Qwen specialize in evidence selection. We
 479 demonstrate that Expert Heads provide interpretable signals for evidence integration, enabling im-
 480 provements in document identification, ranking, and hallucination detection. Beyond performance
 481 gains, they establish a transparent and stable mechanism that links internal model reasoning with
 482 external behavior. Overall, Expert Heads serve both as an interpretability tool and a practical mech-
 483 anism to enhance efficiency, reliability, and controllability in large language models.

486 REFERENCES
487

488 Samira Abnar and Willem Zuidema. Quantifying attention flow in transformers. *arXiv preprint*
489 *arXiv:2005.00928*, 2020.

490 Mistral AI. Mistral-7b-instruct-v0.3, 2024. URL <https://huggingface.co/mistralai/Mistral-7B-Instruct-v0.3>.

491

492 Kevin Clark, Urvashi Khandelwal, Omer Levy, and Christopher D Manning. What does bert look
493 at? an analysis of bert’s attention. *arXiv preprint arXiv:1906.04341*, 2019.

494

495 Andrew Drozdov, Honglei Zhuang, Zhuyun Dai, Zhen Qin, Razieh Rahimi, Xuanhui Wang, Dana
496 Alon, Mohit Iyyer, Andrew McCallum, Donald Metzler, et al. Parade: Passage ranking using
497 demonstrations with large language models. *arXiv preprint arXiv:2310.14408*, 2023.

498

499 Jorge García-Carrasco, Alejandro Maté, and Juan Carlos Trujillo. How does gpt-2 predict acronyms?
500 extracting and understanding a circuit via mechanistic interpretability. In *International Conference on Artificial Intelligence and Statistics*, pp. 3322–3330. PMLR, 2024.

501

502 Qi Guo, Leiyu Wang, Yidong Wang, Wei Ye, and Shikun Zhang. What makes a good order of
503 examples in in-context learning. In *Findings of the Association for Computational Linguistics: ACL 2024*, pp. 14892–14904, 2024.

504

505 Xanh Ho, Anh-Khoa Duong Nguyen, Saku Sugawara, and Akiko Aizawa. Constructing a multi-hop
506 qa dataset for comprehensive evaluation of reasoning steps. *arXiv preprint arXiv:2011.01060*,
507 2020.

508

509 Gautier Izacard, Mathilde Caron, Lucas Hosseini, Sebastian Riedel, Piotr Bojanowski, Armand
510 Joulin, and Edouard Grave. Unsupervised dense information retrieval with contrastive learning.
511 *arXiv preprint arXiv:2112.09118*, 2021.

512

513 Sarthak Jain and Byron C Wallace. Attention is not explanation. *arXiv preprint arXiv:1902.10186*,
514 2019.

515

516 Jeff Johnson, Matthijs Douze, and Hervé Jégou. Billion-scale similarity search with gpus. *IEEE*
517 *Transactions on Big Data*, 7(3):535–547, 2019.

518

519 Vladimir Karpukhin, Barlas Oguz, Sewon Min, Patrick SH Lewis, Ledell Wu, Sergey Edunov, Danqi
520 Chen, and Wen-tau Yih. Dense passage retrieval for open-domain question answering. In *EMNLP*
521 (1), pp. 6769–6781, 2020.

522

523 Omar Khattab and Matei Zaharia. Colbert: Efficient and effective passage search via contextualized
524 late interaction over bert. In *Proceedings of the 43rd International ACM SIGIR conference on*
525 *research and development in Information Retrieval*, pp. 39–48, 2020.

526

527 Omar Khattab, Christopher Potts, and Matei Zaharia. Baleen: Robust multi-hop reasoning at scale
528 via condensed retrieval. *Advances in Neural Information Processing Systems*, 34:27670–27682,
529 2021a.

530

531 Omar Khattab, Christopher Potts, and Matei Zaharia. Relevance-guided supervision for openqa with
532 colbert. *Transactions of the association for computational linguistics*, 9:929–944, 2021b.

533

534 Olga Kovaleva, Alexey Romanov, Anna Rogers, and Anna Rumshisky. Revealing the dark secrets
535 of bert. *arXiv preprint arXiv:1908.08593*, 2019.

536

537 Sreejan Kumar, Theodore R Sumers, Takateru Yamakoshi, Ariel Goldstein, Uri Hasson, Kenneth A
538 Norman, Thomas L Griffiths, Robert D Hawkins, and Samuel A Nastase. Shared functional spe-
539 cialization in transformer-based language models and the human brain. *Nature communications*,
540 15(1):5523, 2024.

541

542 Patrick Lewis, Ethan Perez, Aleksandra Piktus, Fabio Petroni, Vladimir Karpukhin, Naman Goyal,
543 Heinrich Küttler, Mike Lewis, Wen-tau Yih, Tim Rocktäschel, et al. Retrieval-augmented gener-
544 ation for knowledge-intensive nlp tasks. *Advances in neural information processing systems*, 33:
545 9459–9474, 2020.

540 Chaofan Li, Zheng Liu, Shitao Xiao, and Yingxia Shao. Making large language models a better
 541 foundation for dense retrieval. *arXiv preprint arXiv:2312.15503*, 2023a.

542

543 Chong Li, Shaonan Wang, Yunhao Zhang, Jiajun Zhang, and Chengqing Zong. Interpreting and ex-
 544 ploring functional specialization in multi-head attention under multi-task learning. *arXiv preprint*
 545 *arXiv:2310.10318*, 2023b.

546 Nelson F Liu, Kevin Lin, John Hewitt, Ashwin Paranjape, Michele Bevilacqua, Fabio Petroni, and
 547 Percy Liang. Lost in the middle: How language models use long contexts. *arXiv preprint*
 548 *arXiv:2307.03172*, 2023.

549

550 Paul Michel, Omer Levy, and Graham Neubig. Are sixteen heads really better than one? *Advances*
 551 *in neural information processing systems*, 32, 2019.

552 Jianmo Ni, Chen Qu, Jing Lu, Zhuyun Dai, Gustavo Hernandez Abrego, Ji Ma, Vincent Y Zhao,
 553 Yi Luan, Keith B Hall, Ming-Wei Chang, et al. Large dual encoders are generalizable retrievers.
 554 *arXiv preprint arXiv:2112.07899*, 2021.

555 David Patterson, Joseph Gonzalez, Urs Hözle, Quoc Le, Chen Liang, Lluis-Miquel Munguia,
 556 Daniel Rothchild, David R So, Maud Texier, and Jeff Dean. The carbon footprint of machine
 557 learning training will plateau, then shrink. *Computer*, 55(7):18–28, 2022.

558

559 Pouya Pezeshkpour and Estevam Hruschka. Large language models sensitivity to the order of op-
 560 tions in multiple-choice questions. *arXiv preprint arXiv:2308.11483*, 2023.

561 Ofir Press, Noah A Smith, and Mike Lewis. Train short, test long: Attention with linear biases
 562 enables input length extrapolation. *arXiv preprint arXiv:2108.12409*, 2021.

563

564 Danish Pruthi, Mansi Gupta, Bhuwan Dhingra, Graham Neubig, and Zachary C Lipton. Learning
 565 to deceive with attention-based explanations. *arXiv preprint arXiv:1909.07913*, 2019.

566 Jie Ren, Qipeng Guo, Hang Yan, Dongrui Liu, Quanshi Zhang, Xipeng Qiu, and Dahua
 567 Lin. Identifying semantic induction heads to understand in-context learning. *arXiv preprint*
 568 *arXiv:2402.13055*, 2024.

569 Stephen Robertson, Hugo Zaragoza, et al. The probabilistic relevance framework: Bm25 and be-
 570 yond. *Foundations and Trends® in Information Retrieval*, 3(4):333–389, 2009.

571

572 Keshav Santhanam, Omar Khattab, Jon Saad-Falcon, Christopher Potts, and Matei Zaharia.
 573 Colbertv2: Effective and efficient retrieval via lightweight late interaction. *arXiv preprint*
 574 *arXiv:2112.01488*, 2021.

575 Keshav Santhanam, Omar Khattab, Christopher Potts, and Matei Zaharia. Plaid: an efficient en-
 576 gine for late interaction retrieval. In *Proceedings of the 31st ACM International Conference on*
 577 *Information & Knowledge Management*, pp. 1747–1756, 2022.

578

579 Sofia Serrano and Noah A Smith. Is attention interpretable? *arXiv preprint arXiv:1906.03731*,
 580 2019.

581 Qwen Team. Qwen2.5: A party of foundation models, September 2024. URL <https://qwenlm.github.io/blog/qwen2.5/>.

582

583 Curt Tigges, Oskar John Hollinsworth, Atticus Geiger, and Neel Nanda. Linear representations of
 584 sentiment in large language models. *arXiv preprint arXiv:2310.15154*, 2023.

585

586 Harsh Trivedi, Niranjan Balasubramanian, Tushar Khot, and Ashish Sabharwal. Musique: Multihop
 587 questions via single-hop question composition. *Transactions of the Association for Computational*
 588 *Linguistics*, 10:539–554, 2022.

589

590 Jesse Vig. A multiscale visualization of attention in the transformer model. *arXiv preprint*
 591 *arXiv:1906.05714*, 2019.

592

593 Elena Voita, David Talbot, Fedor Moiseev, Rico Sennrich, and Ivan Titov. Analyzing multi-head
 594 self-attention: Specialized heads do the heavy lifting, the rest can be pruned. *arXiv preprint*
arXiv:1905.09418, 2019.

594 Wenhui Wang, Furu Wei, Li Dong, Hangbo Bao, Nan Yang, and Ming Zhou. Minilm: Deep self-
 595 attention distillation for task-agnostic compression of pre-trained transformers. *Advances in neural*
 596 *information processing systems*, 33:5776–5788, 2020.

597 Jason Wei, Xuezhi Wang, Dale Schuurmans, Maarten Bosma, Fei Xia, Ed Chi, Quoc V Le, Denny
 598 Zhou, et al. Chain-of-thought prompting elicits reasoning in large language models. *Advances in neural*
 599 *information processing systems*, 35:24824–24837, 2022.

600 Sarah Wiegreffe and Yuval Pinter. Attention is not explanation. *arXiv preprint arXiv:1908.04626*, 2019.

601 Xinyi Wu, Yifei Wang, Stefanie Jegelka, and Ali Jadbabaie. On the emergence of position bias in
 602 transformers. *arXiv preprint arXiv:2502.01951*, 2025.

603 Shitao Xiao, Zheng Liu, Peitian Zhang, and Xingrun Xing. Lm-cocktail: Resilient tuning of lan-
 604 guage models via model merging. *arXiv preprint arXiv:2311.13534*, 2023.

605 Shitao Xiao, Zheng Liu, Peitian Zhang, Niklas Muennighoff, Defu Lian, and Jian-Yun Nie. C-pack:
 606 Packed resources for general chinese embeddings. In *Proceedings of the 47th international ACM*
 607 *SIGIR conference on research and development in information retrieval*, pp. 641–649, 2024.

608 An Yang, Baosong Yang, Binyuan Hui, Bo Zheng, Bowen Yu, Chang Zhou, Chengpeng Li,
 609 Chengyuan Li, Dayiheng Liu, Fei Huang, Guanting Dong, Haoran Wei, Huan Lin, Jialong Tang,
 610 Jialin Wang, Jian Yang, Jianhong Tu, Jianwei Zhang, Jianxin Ma, Jin Xu, Jingren Zhou, Jinze Bai,
 611 Jinzheng He, Junyang Lin, Kai Dang, Keming Lu, Keqin Chen, Kexin Yang, Mei Li, Mingfeng
 612 Xue, Na Ni, Pei Zhang, Peng Wang, Ru Peng, Rui Men, Ruize Gao, Runji Lin, Shijie Wang, Shuai
 613 Bai, Sinan Tan, Tianhang Zhu, Tianhao Li, Tianyu Liu, Wenbin Ge, Xiaodong Deng, Xiaohuan
 614 Zhou, Xingzhang Ren, Xinyu Zhang, Xipin Wei, Xuancheng Ren, Yang Fan, Yang Yao, Yichang
 615 Zhang, Yu Wan, Yunfei Chu, Yuqiong Liu, Zeyu Cui, Zhenru Zhang, and Zhihao Fan. Qwen2
 616 technical report. *arXiv preprint arXiv:2407.10671*, 2024.

617 Zhilin Yang, Peng Qi, Saizheng Zhang, Yoshua Bengio, William W Cohen, Ruslan Salakhutdinov,
 618 and Christopher D Manning. Hotpotqa: A dataset for diverse, explainable multi-hop question
 619 answering. *arXiv preprint arXiv:1809.09600*, 2018.

620 Peitian Zhang, Shitao Xiao, Zheng Liu, Zhicheng Dou, and Jian-Yun Nie. Retrieve anything to
 621 augment large language models. *arXiv preprint arXiv:2310.07554*, 2023.

622 Peitian Zhang, Zheng Liu, Shitao Xiao, Ninglu Shao, Qiwei Ye, and Zhicheng Dou. Soaring from
 623 4k to 400k: Extending llm’s context with activation beacon. *arXiv preprint arXiv:2401.03462*, 2
 624 (3):5, 2024.

625 Yanzhao Zhang, Mingxin Li, Dingkun Long, Xin Zhang, Huan Lin, Baosong Yang, Pengjun Xie,
 626 An Yang, Dayiheng Liu, Junyang Lin, et al. Qwen3 embedding: Advancing text embedding and
 627 reranking through foundation models. *arXiv preprint arXiv:2506.05176*, 2025.

628 Chujie Zheng, Hao Zhou, Fandong Meng, Jie Zhou, and Minlie Huang. Large language models are
 629 not robust multiple choice selectors. *arXiv preprint arXiv:2309.03882*, 2023.

630 Zifan Zheng, Yezhaohui Wang, Yuxin Huang, Shichao Song, Mingchuan Yang, Bo Tang, Feiyu
 631 Xiong, and Zhiyu Li. Attention heads of large language models: A survey. *arXiv preprint*
 632 *arXiv:2409.03752*, 2024.

633 Honglei Zhuang, Zhen Qin, Kai Hui, Junru Wu, Le Yan, Xuanhui Wang, and Michael Bendersky.
 634 Beyond yes and no: Improving zero-shot llm rankers via scoring fine-grained relevance labels.
 635 *arXiv preprint arXiv:2310.14122*, 2023.

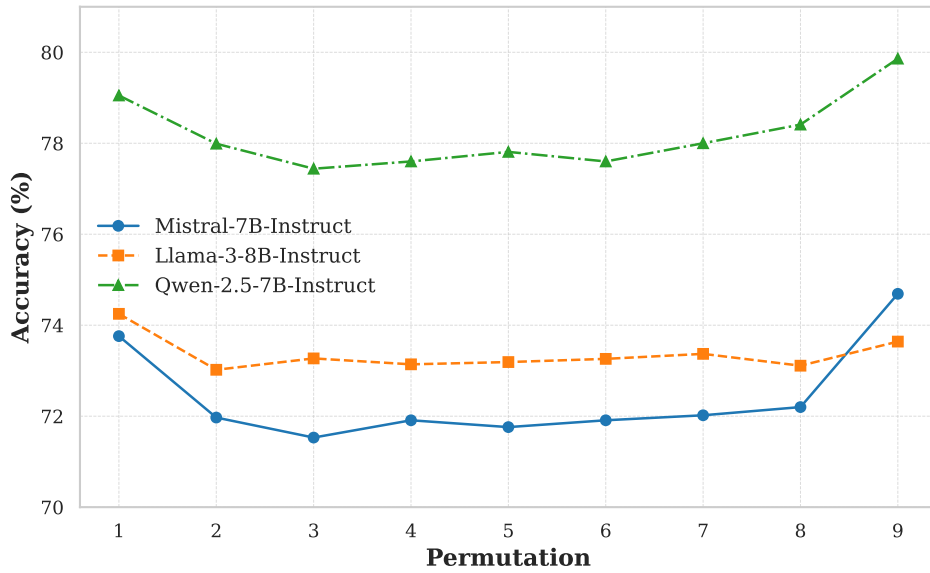
636 Shengyao Zhuang, Xueguang Ma, Bevan Koopman, Jimmy Lin, and Guido Zuccon. Promptreps:
 637 Prompting large language models to generate dense and sparse representations for zero-shot doc-
 638 ument retrieval. *arXiv preprint arXiv:2404.18424*, 2024a.

639 Shengyao Zhuang, Honglei Zhuang, Bevan Koopman, and Guido Zuccon. A setwise approach
 640 for effective and highly efficient zero-shot ranking with large language models. In *Proceedings*
 641 *of the 47th International ACM SIGIR Conference on Research and Development in Information*
 642 *Retrieval*, pp. 38–47, 2024b.

648 A THE USE OF LARGE LANGUAGE MODELS (LLMs)

649
 650 In preparing this paper, **GPT-5-mini** was employed exclusively for **grammar checking and minor**
 651 **language polishing**. No scientific content, experimental design, or interpretation of results was
 652 generated by any LLM. All ideas, analyses, and conclusions presented are solely those of the authors.
 653

654 B IMPLEMENTATION DETAILS



654
 655 Figure 7: Effect of gold document position on multi-hop QA accuracy. The x-axis (1–9) denotes the
 656 gold document’s location, from start (1) to end (9). Accuracy peaks when gold documents are placed
 657 at the beginning or end of the context, and drops when they appear in the middle—demonstrating
 658 strong positional sensitivity in model performance.
 659

660 Table 2: Thresholds and selected Expert Heads for each model and attention source.

Model	Attention Source	(τ_f, τ_p)	Expert Heads (Layer Id, Head Id)
LLaMA-3-8B-Instruct	Question	(0.65, 0.9)	(13,4), (14,13), (14,20), (14,22), (16,1)
LLaMA-3-8B-Instruct	Response	(0.8, 0.9)	(13,18), (14,13), (16,1), (16,8), (17,24)
Mistral-7B-Instruct-v0.3	Question	(0.6, 0.9)	(15,1), (15,27), (16,12), (16,22), (18,3)
Mistral-7B-Instruct-v0.3	Response	(0.75, 0.9)	(15,1), (15,27), (16,12), (18,3), (19,9)
Qwen-2.5-7B-Instruct	Question	(0.6, 0.9)	(16,0), (19,17), (19,20), (19,22), (21,5)
Qwen-2.5-7B-Instruct	Response	(0.8, 0.93)	(19,15), (19,22), (21,5), (22,1), (22,7)

661
 662 Experiments were conducted on 8 NVIDIA V100 GPUs with 32GB memory each. For model
 663 responses, the maximum input length was set to 8192 tokens and the maximum generation length to
 664 4096 tokens with greedy decoding. All retrieval models used a maximum input length of 512 tokens,
 665 while LLM Rank was restricted to a maximum generation length of 30 tokens with greedy decoding.
 666 To ensure reproducibility, all random seeds for model inference, data sampling, and dataset splitting
 667 were fixed at 42.
 668

669 For Expert Head performance evaluation, in order to maintain five heads per category, the activation
 670 frequency and average attention score percentile thresholds were set as shown in Table 2.
 671

672 For threshold sensitivity analysis, the number of selected Expert Heads ranged from 1 to 30.
 673

702 C ALGORITHMIC DETAILS
703
704
705706 **Algorithm 1** Expert Head Selection

707 **Require:** Query Q , Gold Documents $\{G_1, \dots, G_n\}$, Distractor Documents $\{D_1, \dots, D_m\}$, Attention
708 Tensors $A^{(l,h)}$, Activation Frequency Threshold τ_f , Attention Percentile Threshold τ_p
709 **Ensure:** Set of Expert Heads $\mathcal{H}_{\text{expert}}$

710 1: Initialize empty dictionary to store activated heads and their attention scores for all samples and
711 permutations

712 2: **for** each input sample $s \in \mathcal{S}$ **do**

713 3: **for** each input permutation π of documents **do**

714 4: **for** each attention head (l, h) **do**

715 5: **for** each source $src \in \{Q, R\}$ **do**

716 6: Compute attention $A_{src \rightarrow G_j}^{(l,h),s}$ and $A_{src \rightarrow D_i}^{(l,h),s}$ using Eq. 1 or Eq. 2

717 7: Determine activation using Eq. 3

718 8: **end for**

719 9: Store activated heads and their attention scores for later aggregation

720 10: **end for**

721 11: **end for**

722 12: **end for**

723 13: **for** each permutation π and activated head (l, h) **do**

724 14: **for** each source $src \in \{Q, R\}$ **do**

725 15: Compute Activation Frequency $f(l, h)^\pi$ using Eq. 4

726 16: Compute Average Attention $\bar{A}(l, h)^\pi$ using Eq. 5

727 17: **end for**

728 18: **end for**

729 19: Identify Sensitive Heads $\mathcal{H}_{\text{sensitive}}$ using Eq. 6

730 20: Identify Expert Heads $\mathcal{H}_{\text{expert}}$ using Eq. 7

731 21: **return** $\mathcal{H}_{\text{expert}}$

732
733
734 **Algorithm 2** Expert Head Voting for Document Identification and Ranking

735 **Require:** Query Q , Candidate Documents $\{C_1, \dots, C_k\}$, Expert Heads $\mathcal{H}_{\text{expert}}$, Attention Tensors
736 $A^{(l,h)}$, Top- K voting threshold K
737 **Ensure:** Ranked list of documents $\{C_{(1)}, \dots, C_{(k)}\}$

738 1: Initialize vote counts: $V(C_i) \leftarrow 0$ for all $i \in [1, k]$

739 2: **for** each Expert Head $(l, h) \in \mathcal{H}_{\text{expert}}$ **do**

740 3: Compute attention scores $S^{(l,h)}(C_i) \leftarrow A_{Q \rightarrow C_i}^{(l,h)}$ for all i

741 4: Rank documents in descending order of $S^{(l,h)}(C_i)$

742 5: Select top- K documents from this ranking

743 6: **for** each document C_i in top- K **do**

744 7: $V(C_i) \leftarrow V(C_i) + 1$ ▷ This head casts one vote for C_i

745 8: **end for**

746 9: **end for**

747 10: Rank all documents in descending order of $V(C_i)$

748 11: **return** Ranked document list

749
750
751 For clarity and reproducibility, we provide the algorithmic details of the proposed framework in this
752 appendix. Algorithm 1 summarizes the procedure for identifying Expert Heads from raw attention
753 patterns, including input permutations, activation statistics, and consistency checks across different
754 document orderings. Algorithm 2 then illustrates how the selected Expert Heads are leveraged for
755 document identification and ranking, forming the basis of our evaluation experiments in Sec. 4.
Together, these algorithms provide a complete framework for Expert Head selection and evaluation.

756 **D PROMPT TEMPLATES**
757758 This appendix presents the prompt templates used in the experiments for multi-hop question answer-
759 ing and document ranking. Templates are tailored to each model family: LLaMA-3-8B-Instruct,
760 Mistral-7B-Instruct-v0.3, and Qwen-2.5-7B-Instruct.761 Multi-hop QA Templates: Specify structured document inputs followed by a query. The assistant
762 must generate an answer strictly grounded in the provided documents.
763764 Document Ranking Templates: Present 10 candidate documents and a query. The assistant is in-
765 structed to output only a ranked list of document indices, ordered by relevance, without explana-
766 tions.767 These standardized templates ensure consistency across models and tasks, and facilitate repro-
768 ducibility of our experimental results.
769770 **Table 3: Multi-hop Question Answering prompt template for LLaMA-3-8B-Instruct.**
771772 **Multi-hop Question Answering for LLaMA-3-8B-Instruct**
773774 **Input:** <|begin_of_text|><|start_header_id|>system<|end_header_id|>
775 Read the following documents and answer the question based ONLY on the provided information.
776 <|eot_id|><|start_header_id|>user<|end_header_id|>777 Title: ...
778 Content: ...
779780 Title: ...
781 Content: ...
782

783 ...

784 Question: {question}
785 <|eot_id|><|start_header_id|>assistant<|end_header_id|>786 **Output:** {response}787 **Table 4: Multi-hop Question Answering prompt template for Mistral-7B-Instruct-v0.3.**
788789 **Multi-hop Question Answering for Mistral-7B-Instruct-v0.3**
790791 **Input:** <s>[INST]
792 Read the following documents and answer the question based ONLY on the provided information.793 Title: ...
794 Content: ...
795796 Title: ...
797 Content: ...
798799 ...
800 Content: ...
801

802 ...

803 Question: {question}
804 [/INST]805 **Output:** {response}

810
811
812
813
814

Table 5: Multi-hop Question Answering prompt template for Qwen-2.5-7B-Instruct.

815
816
817
818
819
820
821
822
823
824
825
826
827
828
829
830
831
832
833
834
835
836
837
838
839
840

Multi-hop Question Answering for Qwen-2.5-7B-Instruct

Input: <|im_start|>system

Read the following documents and answer the question based ONLY on the provided information.

<|im_end|>

<|im_start|>user

Title: ...

Content: ...

Title: ...

Content: ...

...

Question: {question}

<|im_end|>

<|im_start|>assistant

Output: {response}

839
840

Table 6: Document ranking prompt template for LLaMA-3-8B-Instruct.

841
842
843
844
845
846
847
848
849
850
851
852
853
854
855
856
857
858
859
860
861
862
863

Document ranking for LLaMA-3-8B-Instruct

Input: <|begin_of_text|><|start_header_id|>user<|end_header_id|>

You are an expert document ranker. You are given 10 documents and a question. Rank all documents from most relevant to least relevant in answering the question.

Document [1]:

Title: ...

Content: ...

Document [2]:

Title: ...

Content: ...

...

Question: {question}

Return ONLY a comma-separated list of document numbers, sorted from most relevant to least relevant. Do NOT include any other text or explanation. Example output: 7,3,9,1,5,10,6,2,4,8

<|eot_id|><|start_header_id|>assistant<|end_header_id|>

Output: {ranking list}

864

865

866 Table 7: Document ranking prompt template for Mistral-7B-Instruct-v0.3.
867868 Document ranking for Mistral-7B-Instruct-v0.3
869870 **Input:** <s>[INST]871 You are an expert document ranker. You are given 10 documents and a question. Rank all documents from
872 most relevant to least relevant in answering the question.

873 Document [1]:

874 Title: ...

875 Content: ...

876 Document [2]:

877 Title: ...

878 Content: ...

879 ...

880 Question: {question}

881 Return ONLY a comma-separated list of document numbers, sorted from most relevant to least relevant.
882 Do NOT include any other text or explanation. Example output: 7,3,9,1,5,10,6,2,4,8
883 [/INST]884 **Output:** {ranking list}

885

886

887

888

889

890

891

892 Table 8: Document ranking prompt template for Qwen-2.5-7B-Instruct.
893894 Document ranking for Qwen-2.5-7B-Instruct
895896 **Input:** <|im_start|>system You are Qwen, created by Alibaba Cloud. You are a helpful assistant.
897 <|im_end|>

898 <|im_start|>user

899 You are an expert document ranker. You are given 10 documents and a question. Rank all documents from
900 most relevant to least relevant in answering the question.

901 Document [1]:

902 Title: ...

903 Content: ...

904 Document [2]:

905 Title: ...

906 Content: ...

907 ...

908 Question: {question}

909 Return ONLY a comma-separated list of document numbers, sorted from most relevant to least relevant.
910 Do NOT include any other text or explanation. Example output: 7,3,9,1,5,10,6,2,4,8
911 <|im_end|>

912 <|im_start|>assistant

913 **Output:** {ranking list}

914

915

916

917